Epitaxial growth of ZnO on (1 1 1) Si free of an amorphous interlayer

2014 J. Phys. D: Appl. Phys. 47 105302

(http://iopscience.iop.org/0022-3727/47/10/105302)

IOP Publishing Journal of Physics D: Applied Physics
J. Phys. D: Appl. Phys. **47** (2014) 105302 (6pp) doi:10.1088/0022-3727/47/10/105302

Epitaxial growth of ZnO on (1 1 1) Si free of an amorphous interlayer

Kui Zhang[1,3], Sung Joo Kim[1], Yi Zhang[1], Tassilo Heeg[2], Darrell G Schlom[2,4], Wenzhong Shen[3] and Xiaoqing Pan[1,5]

[1] Department of Materials Science and Engineering, University of Michigan, Ann Arbor, MI 48109, USA
[2] Department of Materials Science and Engineering, Cornell University, Ithaca, NY 14853, USA
[3] Laboratory of Condensed Matter Spectroscopy and Opto-Electronic Physics, and Key Laboratory of Artificial Structures and Quantum Control (Ministry of Education), Department of Physics, Shanghai Jiao Tong University, Shanghai 200240, China
[4] Kavli Institute at Cornell for Nanoscale Science, Ithaca, NY 14853, USA

E-mail: panx@umich.edu

Received 14 November 2013, revised 19 December 2013
Accepted for publication 6 January 2014
Published 13 February 2014

Abstract

Single crystalline (0 0 0 1) ZnO films were grown by pulsed-laser deposition on (1 1 1) Si substrates containing thin Sc_2O_3 buffer layers (1 and 5 nm) which were prepared by molecular-beam epitaxy at 700 °C. Both x-ray diffraction and transmission electron microscopy reveal that the ZnO films grown at 240 and 400 °C are highly crystalline with good epitaxy. The commonly seen amorphous SiO_x layer has been successfully eliminated from the interface between the ZnO/Sc_2O_3 film and (1 1 1) Si substrate, resulting in improved electrical properties. Rectifying effects are observed in the heterojunction exhibiting a turn-on voltage of 1.08 V and an ideality factor of 17.7. The room temperature mobility is 65 $cm^2\ V^{-1}\ s^{-1}$. A donor binding energy of 46.7 meV is determined by temperature-dependent photoluminescence measurements.

Keywords: ZnO, epitaxial growth, STEM, amorphous interlayer, Si

(Some figures may appear in colour only in the online journal)

1. Introduction

As a wide band gap II–VI semiconductor which mainly crystallizes in the hexagonal wurtzite phase, ZnO has a direct band gap of 3.37 and 3.44 eV at room temperature (RT) and 2 K [1], respectively. Its large exciton binding energy (~60 meV) provides an obvious advantage over GaN, ensuring significant excitonic emission at RT. Besides extensive interest in optoelectronic applications over the past years including RT lasing effects from both ZnO thin films [2] and nanowire arrays [3], much attention has also been drawn to carrier transport properties of ZnO [4–6]. Ultraviolet and visible electroluminescence (EL) was demonstrated in a ZnO-based heterostructure at RT [7], and electron dephasing effects have been reported in ZnO at low temperatures, similar to what has been observed in nanocrystalline silicon [8, 9]. Interest in the electrical characteristics of ZnO contributes to the recent rise in activity directed toward growing ZnO on conductive substrates, including the epitaxial growth of ZnO on Si. The latter is also desirable due to the possibility of integrating the promising optoelectronic properties of ZnO with the mature Si industry for multi-functional device applications.

In addition to the obstacles of lattice and thermal expansion, mismatches between ZnO and Si which often lead to polycrystalline or textured ZnO films if directly grown on Si [10], the oxidation of the Si surface into a thin amorphous SiO_x layer is generally seen in most attempts to grow oxides on Si [11]. The mismatch issue can be satisfactorily overcome by intervening buffer materials, including the use of a 30–100 nm thick Sc_2O_3 layer to enable the epitaxial growth of ZnO on (1 1 1) Si [10]. Unfortunately despite the Sc_2O_3 buffer layer the SiO_x layer was still observed [10, figure 2]. Both the buffer layer and this amorphous layer are irrelevant if a device is built on top of the ZnO film. Nevertheless, if the Si substrate is to be utilized as a back contact to form heterojunctions, which is

[5] Author to whom any correspondence should be addressed.

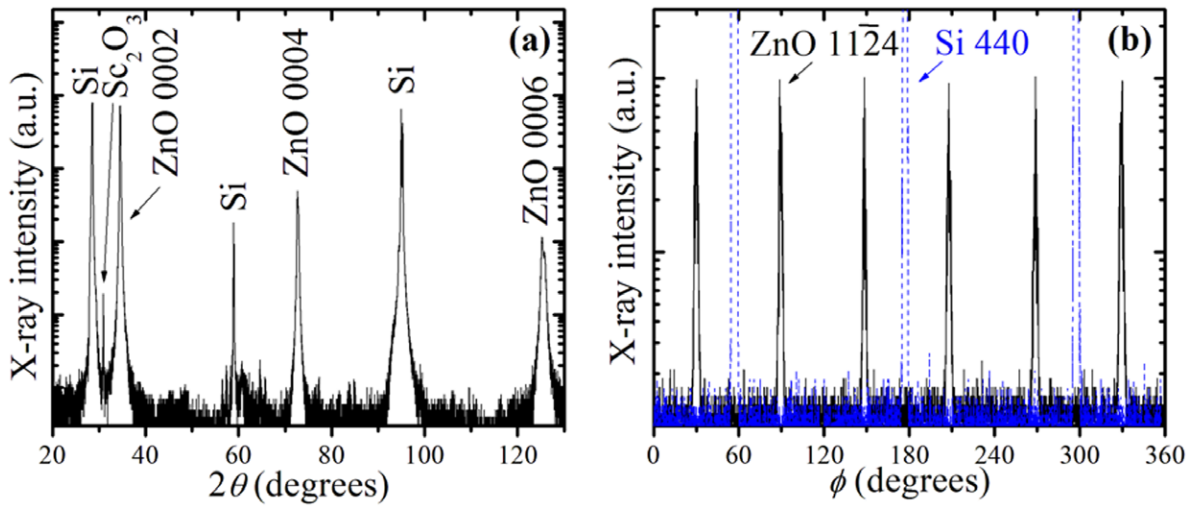

Figure 1. (*a*) Typical θ–2θ XRD pattern of a ∼200 nm thick ZnO film grown on a 1 nm Sc_2O_3 buffer layer on a (1 1 1) Si substrate. A weak Sc_2O_3 peak is seen. The Si peaks originate from the (1 1 1) Si substrate. (*b*) XRD ϕ scan of six-fold ZnO 1 1 $\bar{2}$ 4 (black) and reference Si 440 (blue) peaks.

one of the original intents of growing ZnO on Si, such a thick buffer layer greatly hinders the electronic transport across the junction (as Sc_2O_3 is highly resistive). On the other hand, although a thick insulating SiO_x layer may be desired for some applications, both its thickness and conductivity are harder to control than crystalline buffer layers which can be grown with monolayer precision. A recent study showed that the existence of an amorphous interface layer in a junction structure may give rise to I–V curves with large ideality factors ($n \gg 2.0$) [12], which are frequently observed in ZnO/Si structures. Examples include $n = 32.9$ in a ZnO nanowires/n-Si heterojunction [13], $n = 76.9$ in a ZnO nanorods/p-Si heterojunction [14], and $n = 48.8$ in a ZnO thin film/n-Si LED [7]. While a high ideality factor is usually associated with a high turn-on voltage and a low conduction current, the ability to lower and control this parameter may be vital to designing many practical devices.

In light of the above facts, it is of great importance to minimize the thickness of the insulating buffer layer without jeopardizing the film quality, and to remove the amorphous SiO_x layer. In this paper, we report high quality ZnO films grown at low temperatures (240–400 °C) on Si substrates with very thin Sc_2O_3 buffer layers where the formation of an amorphous SiO_x layer has been successfully avoided, thus realizing a crystalline interface between ZnO and Si. The growth temperature for the ZnO films studied was as low as 240 °C, which is much lower than commonly used growth temperatures (600–900 °C).

2. Experimental

1 and 5 nm thick Sc_2O_3 buffer layers were first grown on (1 1 1) Si substrates by reactive molecular-beam epitaxy (MBE) at 700 °C [10]. Since Sc_2O_3 is thermodynamically stable in contact with Si, the Sc_2O_3/Si interface was abrupt without any reaction phases or amorphous SiO_x layer at this point [11]. A 248 nm KrF excimer laser with a pulse duration of 22 ns and a fluence of ∼1.7 J cm^{-2} was then used for pulsed-laser deposition (PLD) to grow a ZnO nucleation layer approximately 10 nm thick on the buffer material at RT. The temperature of the substrate was subsequently raised to 240 and 400 °C for the growth of ∼200 nm ZnO films in an oxygen ambient of 5×10^{-3} Torr. The substrate-target distance was set to 6.35 cm. The properties of the ZnO films produced in this manner were investigated by x-ray diffraction (XRD) using a Rigaku rotating anode diffractometer with Cu Kα radiation, transmission electron microscopy (TEM), temperature-dependent photoluminescence (PL) excited by a 325 nm Kimmon He–Cd laser and dispersed by a 1 m Jobin-Yvon spectrometer with a photomultiplier tube, and current–voltage (I–V) characterization on a HP 4156 precision semiconductor parameter analyser. Hall effect measurements were performed in Van der Pauw configuration.

3. Results and discussion

3.1. Structural characterization

Figures 1(*a*) and (*b*) are XRD θ–2θ and ϕ scans of a ZnO film grown on 1 nm thick (1 1 1) Sc_2O_3 buffered (1 1 1) Si substrate at 240 °C. These scans reveal the epitaxial growth of Sc_2O_3 on (1 1 1) Si with a B-type orientation relationship. The overall out-of-plane and in-plane orientation relationships are determined as $(0\,0\,0\,1)[1\,\bar{2}\,1\,0]_{ZnO} \parallel (1\,1\,1)[\bar{1}\,1\,0]_{Sc_2O_3} \parallel (1\,1\,1)[1\,\bar{1}\,0]_{Si}$ without any impurity or polycrystalline ZnO peaks detected. The Sc_2O_3 layer was too thin for its diffraction peak to fully emerge in the θ–2θ scan. The six narrow 1 1 $\bar{2}$ 4-type peaks seen in the ϕ-scan (figure 1(*b*)) show that the ZnO film is epitaxial and free of rotation twins. Table 1 lists the full width at half maximum (FWHM) of the 0 0 0 2 ZnO ω-rocking curve measured by high-resolution XRD. A comparison is shown between ∼200 nm thick ZnO samples grown on 1 and 5 nm thick Sc_2O_3 buffer layers on (1 1 1) Si substrates for growth temperatures of 240 and 400 °C. All of these samples have very similar diffraction patterns to those shown in figures 1(*a*) and (*b*). The *c*-type (N_c, mostly dislocations with

Table 1. Comparison of FWHM values of ω-rocking curves and dislocation densities of ZnO films grown at 240 and 400 °C with 1 and 5 nm thick Sc_2O_3 buffer layers.

Substrate with buffer layer	ZnO growth Temperature(°C)	0 0 0 2 FWHM (degrees)	N_c (cm^{-2})	N_a (cm^{-2})
1 nm Sc_2O_3/Si	240	0.56	4.9×10^9	3.4×10^{10}
5 nm Sc_2O_3/Si	240	0.47	3.0×10^9	2.0×10^{10}
1 nm Sc_2O_3/Si	400	0.34	7.8×10^8	5.4×10^9
5 nm Sc_2O_3/Si	400	0.33	5.6×10^8	3.8×10^9

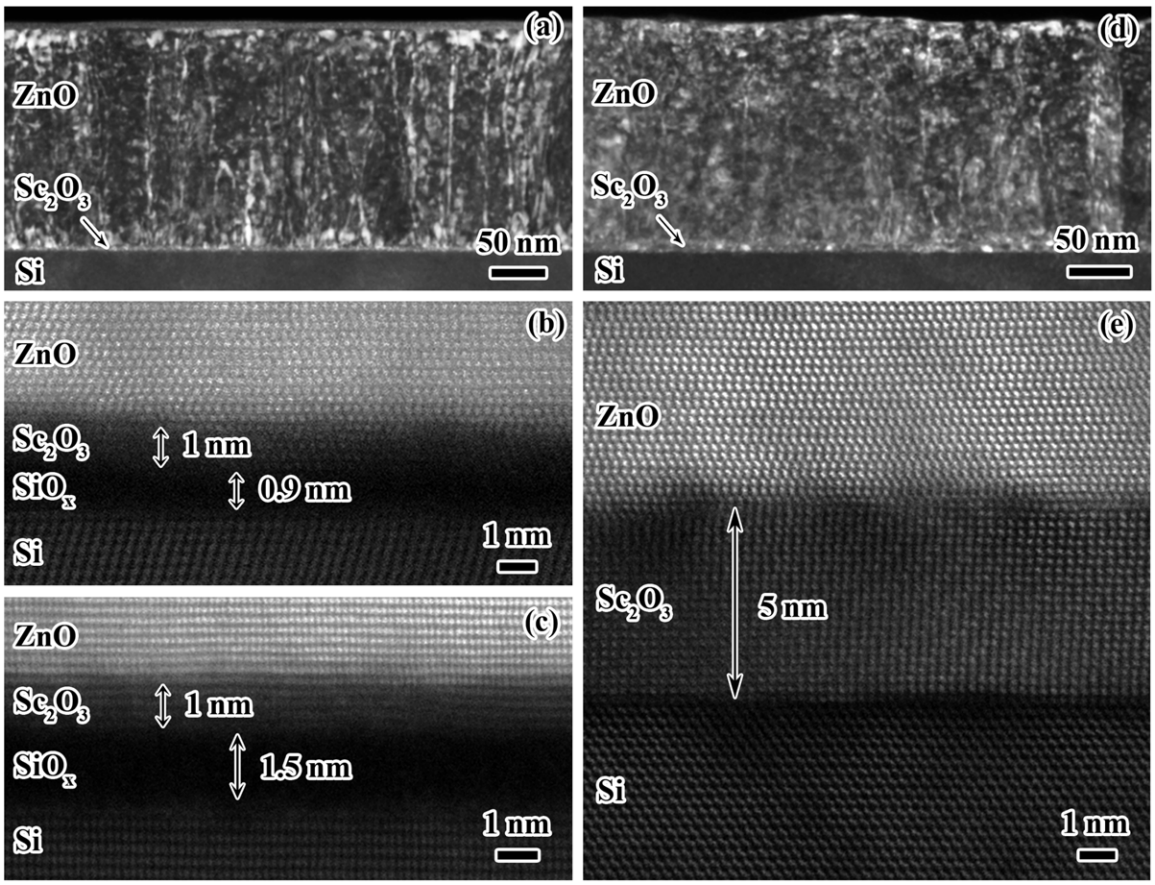

Figure 2. (*a*) Cross-sectional weak-beam dark-field TEM image and (*b*) C_S-corrected HAADF image of a ZnO/Sc_2O_3(1 nm)/Si sample grown at 240 °C. (*c*) HAADF image of a ZnO/Sc_2O_3(1 nm)/Si sample grown at 400 °C. (*d*) Cross-sectional dark-field TEM image and (*e*) HAADF image of a ZnO/Sc_2O_3(5 nm)/Si structure grown at 240 °C.

a screw component) and *a*-type (N_a, mostly edge dislocations) dislocation densities estimated by Hall–Williamson [15] and Srikant off-axis reflection [16] analyses are included in the table, where we see that although lower growth temperature gives rise to increased dislocation densities, the FWHMs have not increased as much. The fact that dislocation densities in films on 5 nm thick Sc_2O_3 buffer layers are generally smaller is easily understood because a thicker buffer layer better mitigates the lattice mismatch and relaxes the strain effects.

Direct characterization of the interfaces in the ZnO/Sc_2O_3/Si multilayer structure was performed by spherical aberration (Cs)-corrected scanning transmission electron microscopy (STEM). Figure 2(*b*) shows a high-angle annular dark-field (HAADF) image taken from the interface between ZnO and Si, revealing good epitaxy of ZnO on Si even though the Sc_2O_3 buffer layer was only 1 nm thick and the growth temperature was merely 240 °C. An amorphous SiO_x layer ~0.9 nm thick exists at the interface of Sc_2O_3 and Si. A cross-sectional weak-beam dark-field TEM image of this sample in figure 2(*a*) reveals a smooth film surface and sharp interface with the substrate. Threading dislocations originating from the interface propagate into ZnO; some of these dislocations extend to the film surface, while several threading dislocations react and terminate within the film. For comparison, figure 2(*d*) shows the cross-sectional TEM image of a ZnO film grown on (1 1 1) Si with a 5 nm thick Sc_2O_3 buffer layer under the same growth conditions; significantly fewer threading dislocations are observed. The dislocation densities calculated from these images are in agreement with those obtained by XRD as listed in table 1. The HAADF image of this ZnO/Sc_2O_3(5 nm)/Si heterostructure is shown in figure 2(*e*), which clearly illustrates the epitaxial growth of

both Sc_2O_3 and ZnO. Most importantly, the Sc_2O_3/Si interface is crystalline and free of an amorphous SiO_x layer. Although a short-range (1–2 atomic layers) reaction is seen between ZnO and Sc_2O_3, this structure presents an extraordinary crystalline interface between ZnO and Si. This is the first epitaxial growth of ZnO on Si that is shown to be free of an amorphous layer.

The elimination of amorphous SiO_x relies on a combination of the growth temperature and the thickness of the buffer layer. High-resolution TEM (HRTEM) images in previous studies showed a Sc_2O_3/Si interface free of SiO_x prior to the film growth, suggesting that the formation of the amorphous layer occurred during the ZnO growth when oxygen from the ambient diffused through Sc_2O_3 and reacted with Si at the interface [10]. At lower growth temperatures the oxygen diffusion coefficient is strongly reduced; similarly a longer diffusion length is needed for oxygen to diffuse through a thicker Sc_2O_3 buffer layer. These concepts are reflected in the results shown in figure 2. A STEM *Z*-contrast image of a ZnO/Sc_2O_3(1 nm)/Si sample grown at a higher temperature (400 °C, other conditions fixed) in figure 2(*c*) shows the SiO_x layer to be 67% thicker than the sample grown at 240 °C in figure 2(*b*). While further reducing the temperature might lead to a compromise of the crystallization quality, increasing the thickness of the buffer layer is another approach according to the above diffusion model. In this work, 240 °C and 5 nm buffer were the proper combination to get rid of amorphous SiO_x. It is foreseeable that other combinations of growth temperature and Sc_2O_3 buffer layer thickness may also preclude the formation of interfacial SiO_x.

3.2. Optical properties

In addition to structural investigation, the optical properties of the ZnO/Sc_2O_3(5 nm)/Si heterostructure grown at 240 °C were examined by temperature-dependent PL measurements. The excitation intensity was set to 5×10^{-2} W cm^{-2}. Figure 3(*a*) shows the near-band-edge (NBE) spectra from 11 to 300 K, where eleven peaks and shoulders are distinguishable on the spectra. Lines at 3.375 and 3.385 eV were identified as the ground state emissions of A and B free excitons ($FX_A^{n=1}$ and $FX_B^{n=1}$), respectively, and the first excited state of the *B* free exciton ($FX_B^{n=2}$) was observed at 3.453 eV [17]. The strongest peak at 3.360 eV and an accompanying shoulder at 3.366 eV were assigned to neutral donor bound exciton recombination (D^0X_A and D^0X_B). $FX_A^{n=1}$ has two longitudinal optical phonon replicas at 3.309 and 3.235 eV, and similarly for D^0X_A its two phonon replicas are located at 3.288 and 3.216 eV. As is frequently seen for ZnO, the donor bound *DX* lines gradually disappear with increasing temperature, while the *FX* lines become significant. The two-electron satellite (TES) transition of D^0X, where the donor final state during the recombination of an exciton bound to a neutral donor is the 2s, 2p state, was determined to be 3.325 eV. Therefore the donor binding energy (E_D) is 4/3 of the energetic distance between D^0X (1s state) and its TES [18], which was precisely calculated to be 46.7 meV. A faint peak at 3.528 eV that is identified as the H-ZnO bond energy [19] denoted by 'H' in figure 3(*a*) has been observed in multiple samples grown under the same conditions, consistent with the neutral hydrogen donor as a common trace impurity in ZnO.

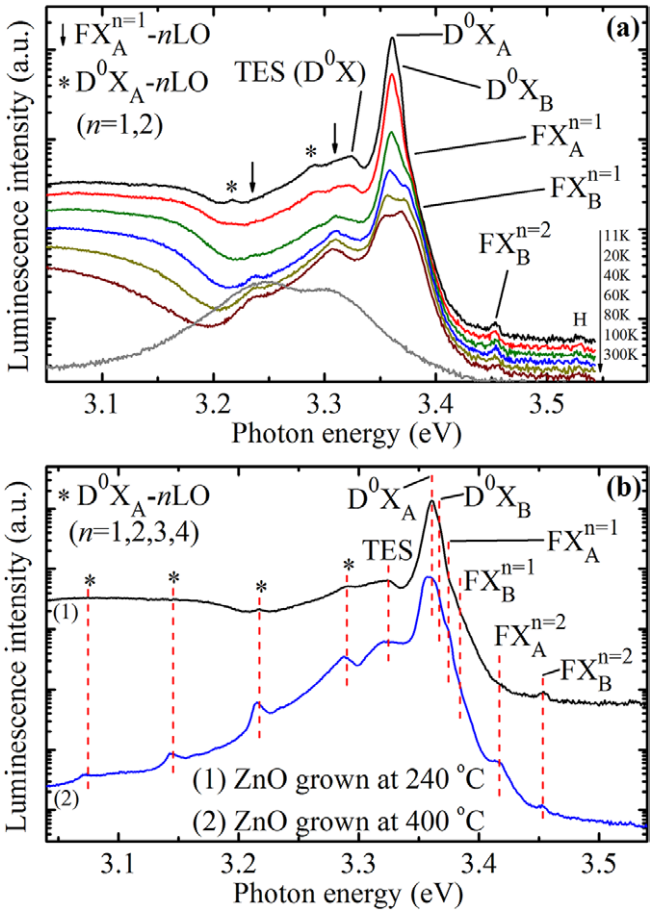

Figure 3. (*a*) Temperature-dependent PL spectra of NBE emissions from a ZnO/Sc_2O_3(5 nm)/Si sample grown at 240 °C. Spectra are vertically displaced for clarity. (*b*) Comparison of 11 K PL spectra of the ZnO film in (*a*) and the other sample grown at 400 °C with other conditions fixed.

Most of the peak positions discussed above exhibit a blueshift of 1–3 meV from their corresponding lines in a ZnO film grown on Sc_2O_3/Si substrate at 600 °C [10], yet there still is a 2–4 meV redshift from those of a ZnO bulk single crystal. Since the redshift in PL spectra is caused by the residual tensile strain [20] induced during the post-growth cooling process due to a mismatch of thermal expansion coefficients between ZnO (6.5×10^{-6} K^{-1}) [21] and Sc_2O_3 (5.2×10^{-6} K^{-1}) [22], the lowered growth temperature has resulted in less strain and hence less redshift. A comparison of this sample with the other ZnO film grown at 400 °C is shown in figure 3(*b*). The higher growth temperature has improved crystallinity and thus the peak resolution; the $FX_A^{n=2}$ line appears at 3.417 eV and more phonon replicas of D^0X_A are visible at 3.146 and 3.075 eV. Note that a slight redshift is present in the 400 °C curve compared with the 240 °C curve, caused by the strain effect.

3.3. Electrical properties

The current-voltage behaviour of the same samples discussed above was examined at RT using indium as a contact material,

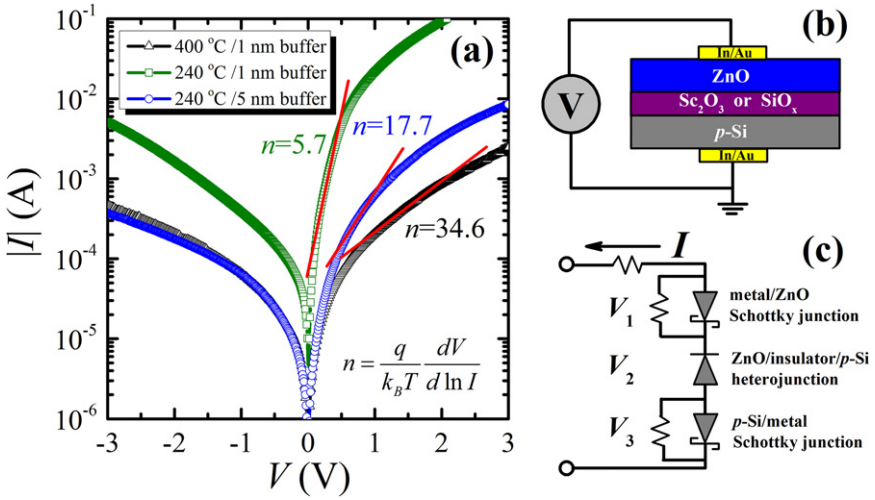

Figure 4. (*a*) Room temperature *I*–*V* characteristics of ZnO/Sc_2O_3/Si heterostructures grown at 240 °C, where the buffer layer thicknesses are 1 nm (square) and 5 nm (circle), respectively, and at 400 °C with 1 nm buffer (triangle). The ideality factors calculated for each sample are shown. (*b*),(*c*) Schematic structure and the equivalent circuit in the interim bias range of the device studied.

to which gold wires were attached on both the ZnO surface and the back of the Si substrate. Si substrates were p-doped with a resistivity of ∼0.02 Ω cm, so they constitute p–n junctions together with the undoped intrinsically n-type ZnO films. Rectifying effects were observed in all samples tested as shown in figure 4(*a*). According to Shockley's ideal diode equation

$$I = I_S(e^{qV/nk_BT} - 1), \tag{1}$$

where I_S is the reverse saturation current and V is the voltage across the junction, the ideality factor n can be written as

$$n = \frac{q}{k_B T}\frac{dV}{d\ln I} \tag{2}$$

and is usually calculated in the interim bias range on the *I*–*V* curve. As marked in figure 4(*a*), in both samples with 1 nm thick Sc_2O_3 buffer layers, the ideality factor dropped greatly from 34.6 to 5.7 when the growth temperature was decreased from 400 to 240 °C, owing to the reduced thickness of the SiO_x layer (see figure 2). Directly linked to the change in ideality factor, the more sensitive 240 °C sample has a turn-on voltage of 0.45 V, much lower than the value of 2.14 V in the 400 °C sample. The structure also grown at 240 °C that is free of the amorphous SiO_x layer has a thicker insulating layer (5 nm Sc_2O_3) than the other two (Sc_2O_3 + SiO_x), but still exhibits a turn-on voltage of 1.08 V and an ideality factor of 17.7, which is lower than most reports on ZnO/Si structures. Because of the apparent advantage of a thin epitaxial Sc_2O_3 crystalline buffer layer over an amorphous SiO_x reaction layer in both structural and electrical qualities, this heterojunction provides among our samples the lowest reverse current, decent sensitivity and forward current, and the best mobility of ∼65 $cm^2\,V^{-1}\,s^{-1}$ from RT Hall measurements, which also show that the ZnO film is n-type with an electron concentration of 6.5×10^{17} cm^{-3}.

An ideality factor much higher than 2 in the Shockley theory can be explained by an equivalent circuit model proposed by Shah *et al* [23] schematically shown in figures 4(*b*) and (*c*). Considering the Schottky contact at In/ZnO and In/Si interfaces, the overall *I*–*V* characteristic of the structure can be expressed as

$$V = \sum_i V_i = \sum_i [n_i(k_BT/q)\ln I - n_i(k_BT/q)\ln I_{S_i}]. \tag{3}$$

Regrouping the expression to get

$$\ln I = \frac{q/k_BT}{\sum_i n_i} V + \frac{\sum_i n_i \ln I_{S_i}}{\sum_i n_i} \tag{4}$$

one can see that the externally calculated ideality factor n of equation (2) is actually the sum of a series of rectifying junctions: $n = \sum_i n_i$, so measuring $n \gg 2.0$ is possible. For future investigation, the junction marked as V_2 in figure 4(*c*) may be resolved into several junctions at each interface. By growing a series of ZnO/Sc_2O_3/(*p*- and *n*-)Si multilayer structures with different intervening layer thicknesses, a systematic study can be conducted to decompose the interfacial effects and further improve the electrical performance.

It should be noted that during experiments on the ZnO/Sc_2O_3 (5 nm)/Si sample, currents up to 500 mA flowed through the junction under forward bias, imposing electrical power larger than 2.3 W on a 20 mm^2 cross section, for over 10 min. Surprisingly neither the thin buffer layer, which endured most of the applied voltage, nor the ZnO crystalline film was damaged by such a high current density, and all measurements were repeatable without degradation, suggesting that the device heating is significantly suppressed compared to structures with oxidized Si layers. Taking the low temperature treatment in PL tests (11 K) into account, this SiO_x-free structure displays excellent stability. Based on the findings in this report, one could design and fabricate more ZnO/Sc_2O_3/Si structures under different conditions to suit the needs of optical or electrical applications.

4. Conclusion

The epitaxial growth of ZnO on (1 1 1) Si, free of an amorphous SiO_x interlayer, has been realized utilizing a 5 nm thick

Sc_2O_3 buffer layer by PLD at a growth temperature of 240 °C. The films grown at such a low temperature maintained high structural and optical quality with superior electrical properties. Rectifying behaviour was observed in the p–n junction with a turn-on voltage of 1.08 V and an ideality factor of 17.7, which may be manipulated by adjusting the growth conditions and Sc_2O_3 buffer layer thickness. It was also demonstrated that a 1 nm Sc_2O_3 buffer layer can already lead to good ZnO epitaxy.

Acknowledgments

This work was supported by the National Science Foundation under Grant No DMR-0907191 and for the work at Cornell Grant No EEC-1160504, and by the Natural Science Foundation of China under contracts 10734020 and 11174202.

References

[1] Look D C, Hemsky J W and Sizelove J R 1999 Residual native shallow donor in ZnO *Phys. Rev. Lett.* **82** 2552–5
[2] Bagnall D M, Chen Y F, Zhu Z, Yao T, Koyama S, Shen M Y and Goto T 1997 *Appl. Phys. Lett.* **70** 2230–2
[3] Huang M H, Mao S, Feick H, Yan H Q, Wu Y Y, Kind H, Weber E, Russo R and Yang P D 2001 *Science* **292** 1897–9
[4] Allenic A, Guo W, Chen Y B, Katz M B, Zhao G Y, Che Y, Hu Z D, Liu B, Zhang S B and Pan X Q 2007 *Adv. Mater.* **19** 3333–7
[5] Ye H B, Kong J F, Shen W Z, Zhao J L and Li X M 2007 *Appl. Phys. Lett.* **90** 102115
[6] Ye H B, Kong J F, Pan W, Shen W Z and Wang B 2009 *Solid State Commun.* **149** 1628–32
[7] Tan S T, Sun X W, Zhao J L, Iwan S, Cen Z H, Chen T P, Ye J D, Lo G Q, Kwong D L and Teo K L 2008 *Appl. Phys. Lett.* **93** 013506
[8] Zhang K and Shen W Z 2008 *Appl. Phys. Lett.* **92** 083101
[9] Zhang K, Hao M R, Guo W, Heeg T, Schlom D G, Shen W Z and Pan X Q 2012 *Physica* B **407** 2825–8
[10] Guo W, Katz M B, Nelson C T, Heeg T, Schlom D G, Liu B, Che Y and Pan X Q 2009 *Appl. Phys. Lett.* **94** 122107
[11] Hubbard K J and Schlom D G 1996 *J. Mater. Res.* **11** 2757–76
[12] Brotzmann M, Vetter U and Hofsass H 2009 *J. Appl. Phys.* **106** 063704
[13] Guo Z, Zhao D X, Liu Y C, Shen D Z, Zhang J Y and Li B H 2008 *Appl. Phys. Lett.* **93** 163501
[14] Liu S Y, Chen T, Jiang Y L, Ru G P and Qu X P 2009 *J. Appl. Phys.* **105** 114504
[15] Williamson G K and Hall W H 1953 *Acta Metall.* **1** 22–31
[16] Srikant V, Speck J S and Clarke D R 1997 *J. Appl. Phys.* **82** 4286–95
[17] Teke A, Ozgur U, Dogan S, Gu X, Morkoc H, Nemeth B, Nause J and Everitt H 2004 *Phys. Rev.* B **70** 195207
[18] Meyer B K *et al* 2004 *Phys. Status Solidi* b **241** 231–60
[19] Sun Q, Xie J J and Zhang T 1994 *Phys. Status Solidi b—Basic Res.* **185** 373–8
[20] Kisielowski C *et al* 1996 *Phys. Rev.* B **54** 17745–53
[21] Albertsson J, Abrahams S C and Kvick A 1989 *Acta Crystallogr.* B **45** 34–40
[22] Stecura S and Campbell W J 1961 *U.S. Bur. Mines. Rep. Invest.* **5847** 14
[23] Shah J M, Li Y L, Gessmann T and Schubert E F 2003 *J. Appl. Phys.* **94** 2627–30